
Taylor series derivation of nonstationary wavefield extrapolators

Gary F. Margrave and Robert J. Ferguson

ABSTRACT

Taylor series expansion of extrapolated wavefields leads directly to the elementary nonstationary wavefield extrapolators *combination* and *convolution*. Other more commonly implemented, extrapolators are derived in this way, and a comparison between them and nonstationary extrapolators is made. Nonstationary combination is found to be equivalent to infinite series implementations of recursive explicit extrapolators (often called ω -x methods), and thus more correctly approximates one-way extrapolation. No existing ω -x analogue is found for nonstationary *convolution*.

The relationship between nonstationary extrapolators and *pseudo-differential* operators provides a basis for error analysis. The errors corresponding to the combination and convolution operators are found to be complimentary. That is, any composition of these operators, resulting in an averaging of their vertical wavenumbers, tends to increase the order of the resulting error and cancels complex values. A new symmetric extrapolator suggested by this analysis, and an existing one (symmetric nonstationary phase shift), are shown to be more accurate and more stable than the elementary extrapolators.

INTRODUCTION

The operators of explicit one-way wavefield extrapolators have recently been recognized as *pseudo-differential* operators (Margrave and Ferguson, 1997; Grimbergen et al., 1998; Margrave and Ferguson, 1999). A pseudo-differential operator is a generalization of translation-invariant (stationary) operators to approximately translation invariant (nonstationary) operators (Stein, 1993). Generalizing a stationary operator, like the constant lateral-velocity phase shift method of Gazdag (1978) to a nonstationary operator, is formulated here as a direct result of Taylor series representation of extrapolated wavefields, and allows extrapolation of seismic wavefields through strongly heterogeneous media. The equivalence of nonstationary wavefield extrapolation and pseudo-differential operators provides access to a large mathematical literature (for introductory texts see Treves, 1980; Peterson, 1983; Stein, 1993) that leads to a better understanding of wavefield extrapolation. After developing the elementary nonstationary extrapolators from Taylor series, we use the general asymptotic formulae of pseudo-differential *composition* operators to examine their accuracy, stability and to help justify the development of two more nonstationary extrapolators that have enhanced accuracy and stability.

Historically, the generalization of stationary phase shift to nonstationary phase shift has been done independently of pseudo-differential operators. For example, in the split-step-Fourier method (Stoffa, et al., 1990) the phase shift operator is split into

a stationary focussing term, and a nonstationary shifting term resulting in good kinematic results that are poorly focussed. Better approximations to the above method are available from Wu (1992) and Wu and Wu (1998). Another nonstationary phase shift method is the phase-shift-plus-interpolation method (PSPI) of Gazdag and Sguazzero (1984). Lateral velocity variation is approximated using a set of constant reference velocities and computing a set of wavefields by stationary phase shift. Each new wavefield corresponds in space to a local constant velocity, and they are interpolated into a single result. Of the methods given above, PSPI corresponds strongly with extrapolation by a single pseudo-differential operator. Margrave and Ferguson (1997; 1999) demonstrate that PSPI in the limit of continuous velocity variation (the nonstationary limit) is equivalent to extrapolation by a pseudo-differential operator. Fishman and McCoy (1985) derive a similar mathematical form but fail to recognize it as PSPI.

Margrave (1998) introduces two forms of nonstationary filters, combination and convolution, in the context of one-dimensional time-variant filtering, and suggests their extension to wavefield extrapolation. Margrave and Ferguson (1997; 1999) develop the combination extrapolator (PSPI in the nonstationary limit) and the convolution extrapolator (nonstationary phase shift: NSPS), and demonstrate the utility of each in depth imaging. Margrave and Ferguson (1998) and Ferguson and Margrave (1999) recognize that PSPI and NSPS are the transpose of one another in the space-frequency domain and can be combined to produce forms that are symmetric in the space domain. Symmetry of explicit extrapolators in the space domain is required by reciprocity considerations (Wapenaar and Grimbergen, 1998).

In this paper, the NSPS and PSPI extrapolators are derived from a Taylor series representation for the extrapolation of a seismic wavefield. For extrapolation from $z = 0$ to z , the Taylor series requires all orders of depth derivatives (evaluated at $z = 0$) of the seismic wavefield. For the second derivative, the Helmholtz equation, with velocity a function of lateral coordinates provides two alternate expressions that are exact for the second partial derivative. These expressions are nonstationary filters of combination and convolution form or, equivalently, pseudo-differential equations in the normal and adjoint forms whose symbols are the square of the vertical wavenumber.

If the assumption is made that the n^{th} derivative is obtained by an equation similar to those for the second derivative, but with a symbol equal to the vertical wavenumber evaluated at the n^{th} power, then two explicit formulae for the Taylor series are obtained. The formula that uses the combination form results in the PSPI extrapolator while the other (the convolution form) gives the NSPS operator. Following Etgen (1994), we demonstrate that PSPI (in the nonstationary limit) is exactly equal to explicit frequency-space (f - x) extrapolation methods implemented as infinitely long finite difference extrapolators, and is therefore more accurate than (f - x) implementations (they use truncated series). Both formulae, NSPS and PSPI, are shown to be approximate but approximate in complementary ways.

By using a theorem for the composition of two pseudo-differential operators we show that the errors made by PSPI tend to cancel those made by NSPS. This suggests

that a new symmetric extrapolator, built by averaging PSPI and NSPS, might be more accurate than either NSPS or PSPI. The direct average of PSPI and NSPS is an explicit extrapolator for complex media that offers advantages in both accuracy and stability over other explicit methods. A similar analysis suggests a fourth operator that is a cascade of NSPS and PSPI. (This symmetric operator was first introduced by Margrave and Ferguson, 1998, and implemented in depth imaging by Ferguson and Margrave, 1999.) A naming convention is introduced to provide simpler and more compact description of nonstationary operators.

A qualitative comparison of the four extrapolators is presented to illustrate their relative accuracy and stability. A wavefield consisting of a null background, in which a number of impulses are embedded, is extrapolated a large distance (200 m) through a strongly varying velocity field. The resulting impulse responses are then reversed through the same field. The two symmetric operators are found to more accurately recover the input through this inversion process. No formal proof is given to establish the equivalence of invertability and accuracy. However, the perfect invertability (in the nonevanescence region) of stationary phase shift suggests that this test is adequate.

Relative stability is demonstrated by singular value decomposition. The extrapolation operators responsible for the forward propagation portion of the preceding experiment are decomposed into their constituent unitary and singular matrices. In the nonevanescence region, only phase changes should be applied to the wavefield, and any singular values that are not equal to unity in this region represent non-physical growth or decay. All four extrapolators are found to be unstable in this way (Etgen, (1994) demonstrates the instability of PSPI), but the two symmetric extrapolators are found to be more stable, and the average operator is the most stable.

THE SEISMIC WAVEFIELD AND NONSTATIONARY FILTERS

A seismic wavefield $\psi(z)$ at depth z in the subsurface is predictable from a wavefield $\psi(0)$ recorded at $z = 0$ by Taylor series (Berkhout, 1981). All orders of the depth derivatives of ψ must be known at $z = 0$. However, from the Helmholtz equation, only the second-depth derivative is exactly known. Two equivalent forms of the second derivative, derived from the Helmholtz equation, are classifiable as *pseudo differential operators* and *nonstationary filters*. This classification leads to the symmetric nonstationary phase-shift extrapolators developed in a later section. For now, we demonstrate that the two equivalent second derivatives give rise to two approximate forms for the first-depth derivative, and thus to two elemental (however not equivalent) forms for all the required depth derivatives. These forms are elemental in that they are the simple and complimentary and can be combined to get higher order extrapolators.

The series expansion of $\psi(z)$, in the z coordinate, gives $\psi(z)$ in terms of a known wavefield, for example $\psi(0)$ recorded at the surface $z = 0$

$$\psi(\mathbf{x}, z) = \psi(\mathbf{x}, 0) + z \left[\frac{\partial}{\partial z} \psi(\mathbf{x}, z) \right]_{z=0} + \frac{z^2}{2} \left[\frac{\partial^2}{\partial z^2} \psi(\mathbf{x}, z) \right]_{z=0} + \dots, \quad (1)$$

where ψ is a monochromatic (in temporal frequency ω) wavefield given in lateral coordinates $\mathbf{x} = \{x, y\}$, and depth coordinate z . Unknown are the depth derivatives $\frac{\partial^n}{\partial z^n}$ of ψ .

An expression for the second depth derivative is found using the Helmholtz equation

$$\frac{\partial^2}{\partial z^2} \psi(\mathbf{x}, z) = - \left[\nabla_{\mathbf{x}}^2 + \left(\frac{\omega}{c(\mathbf{x})} \right)^2 \right] \psi(\mathbf{x}, z), \quad (2)$$

where $\nabla_{\mathbf{x}}^2$ is the Laplacian over the lateral coordinates, and $c(\mathbf{x})$ is the velocity at which ψ propagates. Fourier transform of the Helmholtz equation over \mathbf{x} gives

$$\frac{\partial^2}{\partial z^2} \varphi(\mathbf{k}, z) = - \int \left[\nabla_{\mathbf{x}}^2 + \left(\frac{\omega}{c(\mathbf{x})} \right)^2 \right] \psi(\mathbf{x}, z) \exp(i\mathbf{k} \cdot \mathbf{x}) d\mathbf{x}, \quad (3)$$

where the spectrum φ of ψ is

$$\varphi(\mathbf{k}, z) = \int \psi(\mathbf{x}, z) \exp(i\mathbf{k} \cdot \mathbf{x}) d\mathbf{x}, \quad (4)$$

and $\mathbf{k} = (k_x, k_y)$ are wavenumber coordinates. Computation of the integral in equation (3) (Appendix A) results in an expression for the second depth derivative of φ

$$\frac{\partial^2}{\partial z^2} \varphi(\mathbf{k}, z) = - \int k_z^2(\mathbf{x}, \mathbf{k}) \psi(\mathbf{x}, z) \exp(i\mathbf{k} \cdot \mathbf{x}) d\mathbf{x}, \quad (5)$$

where the square of the vertical wave number k_z is

$$k_z^2(\mathbf{x}, \mathbf{k}) = \left(\frac{\omega}{c(\mathbf{x})} \right)^2 - \mathbf{k} \cdot \mathbf{k}. \quad (6)$$

Equation (5) is an exact prescription for the second z derivative of ψ and is an *adjoint-form* pseudo-differential operator that maps a wavefield ψ to the second-depth derivative of a spectrum φ , and whose *symbol* is $-k_z^2$. It is also a nonstationary *convolution* filter. As a nonstationary filter, equation (5) is classified as a *mixed-domain* filter: the input is a wavefield and the output is a spectrum (Margrave, 1998).

Any nonstationary filters can also be re-expressed in the Fourier and space domains (Margrave, 1998).

Another exact prescription for the second depth derivative is found by substituting for ψ on the right-hand side of equation (2) with the inverse Fourier transform of ϕ

$$\psi(\mathbf{x}, z) = \frac{1}{(2\pi)^2} \int \phi(\mathbf{k}, z) \exp(-i\mathbf{k} \cdot \mathbf{x}) d\mathbf{k} \quad (7)$$

giving for the Helmholtz equation, equation (2),

$$\frac{\partial^2}{\partial z^2} \psi(\mathbf{x}, z) = -\frac{1}{(2\pi)^2} \left[\nabla_{\mathbf{x}}^2 + \left(\frac{\omega}{c(\mathbf{x})} \right)^2 \right] \int \phi(\mathbf{k}, z) \exp(-i\mathbf{k} \cdot \mathbf{x}) d\mathbf{k} \quad (8)$$

The operator contained by the square brackets in equation (8) can be moved inside the Fourier integral (Appendix B) with the result

$$\frac{\partial^2}{\partial z^2} \psi(\mathbf{x}, z) = -\frac{1}{(2\pi)^2} \int k_z^2(\mathbf{x}, \mathbf{k}) \phi(\mathbf{k}, z) \exp(-i\mathbf{k} \cdot \mathbf{x}) d\mathbf{k} \quad (9)$$

Equation (9) is a *pseudo differential operator* (Stein, 1993: 231) that maps a spectrum ϕ to the second-depth derivative of a wavefield ψ , and whose *symbol* is k_z^2 . It is also a *nonstationary combination filter* (Margrave, 1998). Like the convolution filter in equation (5) the combination filter is a mixed domain filter; the input and output are in different Fourier domains. The equivalence of the second derivatives, equations (9) and (5), is shown in Appendix C.

Estimation of all depth derivatives

By inspection, the nonstationary convolution filter of equation (5) suggests that the n^{th} depth derivative is approximately

$$\frac{\partial^n}{\partial z^n} \phi(\mathbf{k}, z) \approx [D_+^n \psi(\mathbf{x}, z)](\mathbf{k}) = \int [\pm i k_z(\mathbf{x}, \mathbf{k})]^n \psi(\mathbf{x}, z) \exp(i\mathbf{k} \cdot \mathbf{x}) d\mathbf{x} \quad (10)$$

where the subscript '+' in the operator D_+^n indicates the operator applies a forward Fourier transform. The vertical wavenumber k_z is

$$k_z(\mathbf{x}, \mathbf{k}) = \sqrt{\left(\frac{\omega}{c(\mathbf{x})} \right)^2 - \mathbf{k} \cdot \mathbf{k}} \quad (11)$$

From the combination filter of equation (9)

$$\frac{\partial^n}{\partial z^n} \psi(\mathbf{x}, z) \approx [D_-^n \phi(\mathbf{k}, z)](\mathbf{x}) = \frac{1}{(2\pi)^2} \int [\pm i k_z(\mathbf{x}, \mathbf{k})]^n \phi(\mathbf{k}, z) \exp(-i\mathbf{k} \cdot \mathbf{x}) d\mathbf{k} \quad (12)$$

where the subscript (-) in derivative operator D_-^n indicates the operator applies an inverse Fourier transform, and k_z is given by equation (11).

In this development it is assumed that velocity is invariant over the depth interval z and, in such a medium, the wavefield is decoupled into downgoing (+) and upgoing (-) modes (Fishman and McCoy, 1985). The desired direction of propagation dictates the choice of sign for k_z for both of equations (10) and (12).

The operators D_-^n and D_+^n provide, equivalently, the exact second derivatives, D_-^2 and D_+^2 , but can only approximate the other others. In the limit of constant v they become exact for all n . In a later section the errors due to using the approximate derivatives D_-^n and D_+^n are characterized and found have opposing tendencies. In the next section, the derivative formulae are shown to give rise to NSPS and PSPI.

SERIES REPRESENTATION OF WAVEFIELD EXTRAPOLATION USING NONSTATIONARY FILTERS

The approximate depth derivatives D_-^n and D_+^n , given above by equations (10) and (12), when used in the series expansion for $\psi(z)$, give rise to two elemental extrapolation methods. Derivative D_-^n leads to the phase-shift-plus-interpolation (PSPI) extrapolator (Gazdag and Sguazzero, 1984) in the limit of continuous lateral variation in velocity (Margrave and Ferguson, 1999). The other, D_+^n , leads to the nonstationary phase shift (NSPS) extrapolator of Margrave and Ferguson (1999).

Returning to the series representation of a wavefield ψ , equation (1), the required n^{th} depth derivatives are replaced by D_-^n

$$\psi(\mathbf{x}, z) = \psi(\mathbf{x}, 0) + z[D_-^1 \phi(\mathbf{k}, 0)](\mathbf{x}) + \frac{z^2}{2}[D_-^2 \phi(\mathbf{k}, 0)](\mathbf{x}) + \dots \quad (13)$$

that can be written explicitly in terms of k_z (using equation (12)) as

$$\psi(\mathbf{x}, z) = \frac{1}{(2\pi)^2} \int \left\{ 1 \pm izk_z(\mathbf{x}, \mathbf{k}) + \frac{i^2 z^2}{2} k_z^2(\mathbf{x}, \mathbf{k}) \pm \dots \right\} \phi(\mathbf{k}, 0) \exp(-i\mathbf{k} \cdot \mathbf{x}) d\mathbf{k} \quad (14)$$

where the first term in equation (13) has been replaced by the inverse Fourier transform of ϕ , and the resulting infinite series of inverse Fourier transforms is collected under a single transform. Recognizing the series expansion for the exponential function (the term in the curly braces) equation (14) becomes

$$\psi(\mathbf{x}, z) = [L_p^\pm \phi(\mathbf{k}, 0)](\mathbf{x}) = \frac{1}{(2\pi)^2} \int \alpha(\mathbf{x}, \mathbf{k}, \pm z) \phi(\mathbf{k}, 0) \exp(-i\mathbf{x} \cdot \mathbf{k}) d\mathbf{k} \quad (15)$$

where linear operator L_p^\pm is introduced. In this operator notation, subscript P stands for PSPI, and the superscript determines the direction of propagation along the depth coordinate. The symbol of this pseudo-differential operator is

$$\alpha(\mathbf{k}, \pm z) = \exp(\pm izk_z(\mathbf{x}, \mathbf{k})) \quad (16)$$

where k_z is given by equation (11). Linear operator L_p^\pm applies the mixed domain form of a nonstationary filter known to be PSPI in the limit of continuous lateral variation in velocity (Margrave and Ferguson, 1999). It is also a standard form pseudo-differential operator (Stein, 1993: 231).

Fishman and McCoy (1985) develop the same limiting form of PSPI as a generalization of wave propagation in a homogeneous medium to a heterogeneous medium. They characterize it as a high frequency approximation (Fishman and McCoy, 1985).

The development of a second expression for wavefield extrapolation using D_+^n (equation (10)) requires the Fourier transform of the series representation of ψ (equation (1))

$$\varphi(\mathbf{k}, z) = \varphi(\mathbf{k}, 0) + z \left[\frac{\partial}{\partial z} \varphi(\mathbf{k}, z) \right]_{z=0} + \frac{z^2}{2} \left[\frac{\partial^2}{\partial z^2} \varphi(\mathbf{k}, z) \right]_{z=0} + \dots \quad (17)$$

Replacing the depth derivatives in equation (17) with D_+^n gives

$$\varphi(\mathbf{k}, z) = \varphi(\mathbf{k}, 0) + z [D_+^1 \psi(\mathbf{x}, z)](\mathbf{k}) + \frac{z^2}{2} [D_+^2 \psi(\mathbf{x}, z)](\mathbf{k}) + \dots \quad (18)$$

that is written in explicit terms of k_z as

$$\varphi(\mathbf{k}, z) = \int \left\{ 1 \pm izk_z(\mathbf{x}, \mathbf{k}) + \frac{i^2 z^2}{2} k_z^2(\mathbf{x}, \mathbf{k}) \pm \dots \right\} \psi(\mathbf{x}, 0) \exp(i\mathbf{k} \cdot \mathbf{x}) d\mathbf{x} \quad (19)$$

The lead term $\varphi(z = 0)$, in equation (18), has been replaced by the Fourier transform of ψ , and the resulting infinite series of Fourier transforms is collected under a single transform. Again, recognizing the series expansion for the exponential, equation (19) becomes

$$\varphi(\mathbf{k}, z) = [L_N^\pm \psi(\mathbf{x}, 0)](\mathbf{k}) = \int \alpha(\mathbf{x}, \mathbf{k}, \pm z) \psi(\mathbf{x}, 0) \exp(i\mathbf{k} \cdot \mathbf{x}) d\mathbf{x} \quad (20)$$

with α given by equation (16). Linear operator L_N^\pm is the mixed domain form of a nonstationary wavefield extrapolator known as NSPS (Margrave and Ferguson, 1999). It is also the adjoint form pseudo-differential operator (Margrave and Ferguson, 1999).

COMPARISON OF PSPI TO EXPLICIT FINITE DIFFERENCE (x- ω) METHODS

Implementation of nonstationary wavefield extrapolation can be done explicitly and without further approximation; this topic will be examined later. For the present it is necessary, for greater understanding, to compare nonstationary methods with familiar explicit methods like finite difference. As will be shown, finite difference methods extend naturally from the nonstationary filter methods presented above.

In two spatial dimensions (x, z) the symbol k_z (equation (11)) of depth derivative D_z^1 (equation (12) with $n = 1$) is expanded as

$$k_z(x, k_x) = \frac{\omega}{c(x)} \left[1 - \frac{1}{2} \left(\frac{c(x)}{\omega} \right)^2 k_x^2 + \frac{1}{8} \left(\frac{c(x)}{\omega} \right)^4 k_x^4 - \dots \right]. \quad (21)$$

Recognizing that $\frac{\partial}{\partial x^2} \Leftrightarrow k_x^2$ leads to a series expression for D_z^n

$$[D_z^1 \psi(x, z)](x) = \pm \frac{\omega}{c(x)} \left[1 + \frac{1}{2} \left(\frac{c(x)}{\omega} \right)^2 \frac{\partial}{\partial x^2} - \frac{1}{8} \left(\frac{c(x)}{\omega} \right)^4 \frac{\partial}{\partial x^4} + \dots \right] \psi(x, z), \quad (22)$$

where the series representation has been moved outside of the integral and the inverse Fourier transform of ϕ has been computed (Berkhout, 1981). In practice, the spatial derivatives are approximated by finite difference operators and the series in square brackets is truncated (Claerbout, 1976). Extrapolation of wavefield ψ then proceeds by equation (1) where the required orders of depth derivatives are computed using appropriate applications of equation (22). Equation (1) must be truncated to a tractable number of terms as well. Modern implementations use better approximations to the square root and increasing numbers of terms in the series (see for example Holberg, 1988; Blacquiere et al., 1989; Hale, 1991a, 1991b; Soubras, 1992).

Wavefield extrapolation by finite differences is developed directly from the nonstationary filter of equation (12) and three levels of approximation are uncovered: the truncation of the square root, the truncation of the Laplacian, and the truncation of the series representing the wavefield. These three approximations are in addition to those of nonstationary methods; thus, a nonstationary phase shift implementation will always be more accurate than the finite difference methods defined here. However, the increased accuracy of nonstationary methods comes at the expense of increased computational effort.

The first depth derivative expression used to develop the finite difference method also leads directly to PSPI (in the limit of continuous lateral velocity variation), (equation (15)). Therefore, the limiting form of PSPI is equivalent to an infinite series representation of the finite difference method. Etgen (1994) has also observed the equivalence of PSPI and finite differences.

ERROR ASSOCIATED WITH NSPS AND PSPI

The wavefield extrapolators L_N^\pm (NSPS, equation (20)) and L_p^\pm (PSPI, equation (15)) follow from two approximate forms of the n^{th} depth derivatives D_+^n (equation (10)) and D_-^n (equation (12)). It is natural to compare the exact second derivatives (equations (5) and (9)) to those that arise from two applications of the approximate first derivatives D_+^1 and D_-^1 . This comparison reveals error terms in both approximations that are complex valued, and have opposing trends.

Beginning with D_+^1 the approximate second derivative is

$$\frac{\partial^2}{\partial z^2} \varphi(\mathbf{k}, z) \approx [D_+^1 D_+^1 \psi(\mathbf{y}, z)](\mathbf{k}) = - \int \hat{k}_z^2(\mathbf{y}, \mathbf{k}) \psi(\mathbf{y}, z) \exp(i\mathbf{k} \cdot \mathbf{y}) d\mathbf{y} \quad (23)$$

where symbol \hat{k}_z^2 is (Appendix D)

$$\hat{k}_z^2(\mathbf{y}, \mathbf{k}) = \frac{1}{(2\pi)^2} \iint k_z(\mathbf{x}, \mathbf{k}) k_z(\mathbf{y}, \mathbf{m}) \exp(i[\mathbf{m} - \mathbf{k}] \cdot [\mathbf{y} - \mathbf{x}]) d\mathbf{m} d\mathbf{x} \quad (24)$$

From D_-^1 the approximate second derivative is

$$\frac{\partial^2}{\partial z^2} \psi(\mathbf{x}, z) \approx [D_-^1 D_-^1 \varphi(\mathbf{m}, z)](\mathbf{x}) = - \frac{1}{(2\pi)^2} \int \bar{k}_z^2(\mathbf{x}, \mathbf{m}) \varphi(\mathbf{m}, z) \exp(-i\mathbf{m} \cdot \mathbf{x}) d\mathbf{m} \quad (25)$$

where symbol \bar{k}_z^2 is (following a procedure analogous to Appendix D)

$$\bar{k}_z^2(\mathbf{x}, \mathbf{m}) = \frac{1}{(2\pi)^2} \iint k_z(\mathbf{x}, \mathbf{k}) k_z(\mathbf{y}, \mathbf{m}) \exp(i[\mathbf{m} - \mathbf{k}] \cdot [\mathbf{x} - \mathbf{y}]) d\mathbf{y} d\mathbf{k} \quad (26)$$

Equations (23) and (25) are pseudo-differential equations with symbols \hat{k}_z^2 and \bar{k}_z^2 that map wavefield ψ (equation (23)) and spectrum φ (equation (25)) to their approximate second depth derivatives simultaneous with a change in Fourier domain. Note, \hat{k}_z^2 and \bar{k}_z^2 are functions of different spatial variables; \hat{k}_z^2 depends upon the input lateral coordinates, while \bar{k}_z^2 depends upon the output coordinates. Further, their symbols, \hat{k}_z^2 and \bar{k}_z^2 , are composed of symbols $k_z(\mathbf{x}, \mathbf{k})$ and $k_z(\mathbf{y}, \mathbf{k})$. A general theorem for this *composition* of symbols (Stein, 1993: 237-238, or Taylor, 1996: 11-13) can be used to provide asymptotic formulae for \hat{k}_z^2 and \bar{k}_z^2 . From Appendix D the formulae are

$$\begin{aligned} \hat{k}_z^2(\mathbf{x}, \mathbf{m}) &= k_z^2(\mathbf{x}, \mathbf{m}) - i \nabla_{\mathbf{m}} k_z(\mathbf{x}, \mathbf{m}) \cdot \nabla_{\mathbf{x}} k_z(\mathbf{x}, \mathbf{m}) \\ &+ \frac{i^2}{2} \nabla_{\mathbf{m}} \nabla_{\mathbf{m}} k_z(\mathbf{x}, \mathbf{m}) : \nabla_{\mathbf{x}} \nabla_{\mathbf{x}} k_z(\mathbf{x}, \mathbf{m}) - \dots \end{aligned} \quad (27)$$

and,

$$\begin{aligned} \bar{k}_z^2(\mathbf{x}, \mathbf{m}) &= k_z^2(\mathbf{x}, \mathbf{m}) + i \nabla_{\mathbf{m}} k_z(\mathbf{x}, \mathbf{m}) \cdot \nabla_{\mathbf{x}} k_z(\mathbf{x}, \mathbf{m}) \\ &+ \frac{i^2}{2} \nabla_{\mathbf{m}} \nabla_{\mathbf{m}} k_z(\mathbf{x}, \mathbf{m}) : \nabla_{\mathbf{x}} \nabla_{\mathbf{x}} k_z(\mathbf{x}, \mathbf{m}) + \dots \end{aligned} \quad (28)$$

The first terms in these asymptotic forms reproduce the action of the exact second-depth derivative. However, terms of higher order represent error, and the odd valued terms are complex. Generation of complex terms by application of D_+^1 or D_-^1 may explain the instability of L_p^\pm observed by Etgen (1994) and, as will be shown, the equivalent instability of L_N^\pm . Uncontrolled complex values in the exponent k_z of α (equation (16)) can lead to instability during recursive application.

The validity of these asymptotic series requires the existence of all orders of spatial and wavenumber derivatives of k_z as given by equation (11). The wavenumber derivatives will exist to all orders except possibly at the evanescent boundary. The spatial derivatives impose a condition of smoothness upon $c(\mathbf{x})$. This condition is not necessarily required for the NSPS and PSPI extrapolators themselves, but it is needed for this form of error analysis.

SYMMETRIC NONSTATIONARY PHASE SHIFT OPERATORS

In this section, two new nonstationary extrapolators L_A^\pm and L_{PN}^\pm are developed that are more accurate and more stable than L_p^\pm and L_N^\pm . The accuracy and stability of the *average* extrapolator, L_A^\pm , is the result of averaging L_p^\pm and L_N^\pm as suggested by the depth-derivative analysis above to reduce error and improve stability. The second extrapolator, L_{PN}^\pm , is the result of recognizing the complimentary nature of L_p^\pm and L_N^\pm : L_N^\pm carries a wavefield ψ to a spectrum ϕ , and L_p^\pm carries a spectrum ϕ to a wavefield ψ . Both extrapolators, at some level, average the vertical wavenumbers k_z corresponding to L_p^\pm and L_N^\pm , resulting in greater accuracy and stability (shown in the next section).

Assuming that error decreases with increasing order in their series, then the average of their symbols, \hat{k}_z^2 and \bar{k}_z^2

$$\frac{\hat{k}_z^2(\mathbf{x}, \mathbf{m}) + \bar{k}_z^2(\mathbf{x}, \mathbf{m})}{2} = k_z^2(\mathbf{x}, \mathbf{m}) + \frac{i^2}{2} \nabla_{\mathbf{m}} \nabla_{\mathbf{m}} k_z(\mathbf{x}, \mathbf{m}) : \nabla_{\mathbf{x}} \nabla_{\mathbf{x}} k_z(\mathbf{x}, \mathbf{m}) + \dots \quad (29)$$

may have greater accuracy due to cancellation of every other term. Note also that the average symbol is always real valued (i.e., the complex terms have canceled). The above suggests that the depth derivatives required by equation (1) may be more stable and more accurately computed by averaging derivatives D_-^n and D_+^n . (A complete analysis would require characterizing the errors involved with all orders of depth derivatives. We do not attempt that here.) Equation (1) is then written

$$\begin{aligned} \psi(\mathbf{x}, z) = & \psi(\mathbf{x}, 0) + \frac{1}{2} z \left[[D_-^1 \phi(\mathbf{k}, z)](\mathbf{x}) + \frac{1}{(2\pi)^2} \int [D_+^1 \psi(\mathbf{x}, z)](\mathbf{k}) \exp(-i\mathbf{k} \cdot \mathbf{x}) d\mathbf{k} \right]_{z=0} \\ & + \frac{1}{2} \frac{z^2}{2} \left[[D_-^2 \phi(\mathbf{k}, z)](\mathbf{x}) + \frac{1}{(2\pi)^2} \int [D_+^2 \psi(\mathbf{x}, z)](\mathbf{k}) \exp(-i\mathbf{k} \cdot \mathbf{x}) d\mathbf{k} \right]_{z=0} + \dots \end{aligned} \quad (30)$$

where derivatives corresponding to D_+^n are inverse Fourier transformed prior to averaging with those corresponding to D_-^n . Collecting terms, writing the derivatives explicitly in k_z , and recognizing the series representation of the exponential reduces equation (30) to the average of the output of L_p^\pm and the inverse Fourier transform of the output of L_N^\pm

$$\psi(\mathbf{x}, z) = \frac{1}{2} \left[\frac{1}{(2\pi)^2} \int \alpha(\mathbf{x}, \mathbf{k}, z) \phi(\mathbf{k}, z) \exp(-i\mathbf{k} \cdot \mathbf{x}) d\mathbf{k} + \frac{1}{(2\pi)^2} \iint \alpha(\mathbf{y}, \mathbf{k}, z) \psi(\mathbf{y}, z) \exp(-i\mathbf{k} \cdot [\mathbf{x} - \mathbf{y}]) d\mathbf{y} d\mathbf{k} \right]. \quad (31)$$

Replacing ϕ in equation (31) with the Fourier transform of ψ and collecting terms results in the following pseudo-differential equation

$$\begin{aligned} \psi(\mathbf{x}, z) = & [L_A^\pm \psi(\mathbf{y}, 0)](\mathbf{x}) = \\ & \int \psi(\mathbf{y}, 0) \frac{1}{(2\pi)^2} \int [\alpha(\mathbf{x}, \mathbf{k}, \pm z) + \alpha(\mathbf{y}, \mathbf{k}, \pm z)] \exp(-\mathbf{k} \cdot [\mathbf{x} - \mathbf{y}]) d\mathbf{k} d\mathbf{y}. \end{aligned} \quad (32)$$

Unlike L_N^\pm and L_P^\pm , L_A^\pm is symmetric under the exchange of coordinates \mathbf{x} and \mathbf{y} .

A fourth extrapolator that is also symmetric is a cascade of L_N^\pm and L_P^\pm . Beginning with L_N^\pm , extrapolate ψ through half the depth interval $z/2$

$$\left[L_N^{\pm \frac{1}{2}} \psi(\mathbf{y}, 0) \right](\mathbf{k}) = \int \alpha \left(\mathbf{y}, \mathbf{k}, \pm \frac{z}{2} \right) \psi(\mathbf{y}) \exp(i\mathbf{k} \cdot \mathbf{y}) d\mathbf{y} \quad (33)$$

and extrapolate the resulting spectrum $\varphi_{z/2}$ through the remaining depth interval $z/2$

$$\left[L_P^{\pm \frac{1}{2}} L_N^{\pm \frac{1}{2}} \psi(\mathbf{y}, 0) \right](\mathbf{x}) = \int \alpha \left(\mathbf{x}, \mathbf{k}, \pm \frac{z}{2} \right) \int \alpha \left(\mathbf{y}, \mathbf{k}, \pm \frac{z}{2} \right) \psi(\mathbf{y}) \exp(i\mathbf{k} \cdot \mathbf{y}) d\mathbf{y} \exp(-i\mathbf{k} \cdot \mathbf{x}) d\mathbf{k} \quad (34)$$

Upon switching the order of integration a new extrapolator L_{PN}^{\pm} is defined

$$\begin{aligned} \left[L_{PN}^{\pm} \psi(\mathbf{y}, 0) \right](\mathbf{x}) &= \left[L_P^{\pm \frac{1}{2}} L_N^{\pm \frac{1}{2}} \psi(\mathbf{y}, 0) \right](\mathbf{x}) \\ &= \int \psi(\mathbf{y}) \int \alpha \left(\mathbf{x}, \mathbf{k}, \pm \frac{z}{2} \right) \alpha \left(\mathbf{y}, \mathbf{k}, \pm \frac{z}{2} \right) \exp(-i\mathbf{k} \cdot [\mathbf{x} - \mathbf{y}]) d\mathbf{k} d\mathbf{y} \end{aligned} \quad (35)$$

The subscript in L_{PN}^{\pm} indicates $L_N^{\pm \frac{1}{2}}$ is applied first, followed by $L_P^{\pm \frac{1}{2}}$.

Like L_A^{\pm} , L_{PN}^{\pm} is symmetric under an exchange of coordinates \mathbf{x} and \mathbf{y} . (A fifth operator L_{NP}^{\pm} would extrapolate spectra instead of wavefields.) Multiplication of the symbols α in equation (35) averages their respective vertical wavenumbers k_z suggesting that, like L_A^{\pm} , L_{PN}^{\pm} can be expected to be more accurate and have greater stability than L_N^{\pm} and L_P^{\pm} .

The average extrapolator L_A^{\pm} and the cascade operator L_{PN}^{\pm} are symmetric explicit extrapolators suitable for 2D or 3D depth imaging. Wapenaar and Grimbergen (1998) use reciprocity concepts to argue that accurate extrapolators should be symmetric in the (\mathbf{x}, ω) domain. We note that ordinary phase shift has such symmetry. Many other symmetric forms, beyond the scope of this paper, are possible including the Weyl form, which uses symbol $\alpha \left(\frac{\mathbf{x} + \mathbf{y}}{2}, \mathbf{k}, z \right)$.

THE ACCURACY AND STABILITY OF NONSTATIONARY PHASE SHIFT EXTRAPOLATORS

Extrapolators L_P^+ , L_N^+ , L_A^+ and L_{PN}^+ are assessed by first computing then inverting their respective impulse responses, and by examining their singular value matrices. This is done for a large extrapolation distance (200m) through a strongly variable velocity field. In the inversion experiment the most accurate extrapolators, L_A^+ and L_{PN}^+ , return the best images of the input. (This direct relationship between

invertability and accuracy is not strictly proven but is inferred by analogy with the perfectly invertable stationary phase shift.) The most stable extrapolators, again L_A^+ and L_{PN}^+ , have singular values closest to unity in the nonevanescient region. Relative stabilities are established because, over a large number of recursions, singular values not equal to unity will cause nonphysical growth or decay of the wavefield.

Figures 2a and 2b show the impulse responses $L_N^+ \psi_{imp}$ and $L_P^+ \psi_{imp}$ for extrapolation of the impulses ψ_{imp} , Figure 1a, through the velocity profile of Figure 1b. The velocity profile is a step function and two characteristic types of extrapolated wave energy are expected; one corresponding to the slow velocity on the right, and one for the fast velocity on the left. In Figure 2a, $L_N^+ \psi_{imp}$, the two types of wave energy are continuously superimposed, but there is no refraction at the velocity boundary. This is in contrast to the discontinuous superposition with change in slope at the velocity boundary provided by $L_P^+ \psi_{imp}$ (Figure 2b).

Accuracy

Conducting the same experiment as above, but using the rapidly varying profile of Figure 3, produces the impulse responses $L_N^+ \psi_{imp}$ and $L_P^+ \psi_{imp}$ in Figures 4a and 4b. Note how the characteristics of $L_N^+ \psi_{imp}$ and $L_P^+ \psi_{imp}$ are retained: $L_N^+ \psi_{imp}$ gives a smooth superposition and $L_P^+ \psi_{imp}$ gives discontinuous superposition.

Inversion of impulse responses $L_N^- L_N^+ \psi_{imp}$ and $L_P^- L_P^+ \psi_{imp}$, Figures 4a and 4b, are given in Figures 5a and 5b. (The data of Figures 4a and 4b are extrapolated $-200m$.) Ideally, in the nonevanescient region, ψ_{imp} is resolved but because L_N^+ and L_P^+ are approximate extrapolators, reversing the direction of propagation does not restore the input. As $z \rightarrow 0$ $L_N^+ \psi_{imp}$ and $L_P^+ \psi_{imp}$ become perfectly invertable (not shown).

The impulse responses $L_{PN}^+ \psi_{imp}$ and $L_A^+ \psi_{imp}$ for extrapolation of the data in Figures 1a and 1b are given in Figures 6a and 6b. For $L_{PN}^+ \psi_{imp}$, note how the discontinuous appearance of $L_P^+ \psi_{imp}$ has been combined with that of the continuous appearance $L_N^+ \psi_{imp}$. Impulse response $L_A^+ \psi_{imp}$ is clearly the average of $L_N^+ \psi_{imp}$ and $L_P^+ \psi_{imp}$.

For the rapidly varying profile of Figure 3 impulse responses $L_{PN}^+ \psi_{imp}$ and $L_A^+ \psi_{imp}$ are given in Figures 7a and 7b. Arrows are annotated to indicate where obvious points of comparison are found. These points show that the characteristic averaged appearance of $L_A^+ \psi_{imp}$ and the combined appearance of $L_{PN}^+ \psi_{imp}$ are preserved. Inversions of these data, $L_{PN}^- L_{PN}^+ \psi_{imp}$ and $L_A^- L_A^+ \psi_{imp}$, are given in Figures 8a and 8b.

Unlike $L_N^- L_N^+ \Psi_{imp}$ and $L_P^- L_P^+ \Psi_{imp}$, inversion of the symmetric operators $L_{PN}^- L_{PN}^+ \Psi_{imp}$ and $L_A^- L_A^+ \Psi_{imp}$ provide good images of Ψ_{imp} .

Because constant velocity phase shift has the attributes of perfect accuracy and invertability in the nonevanescence zone, the more accurate nonstationary extrapolator should demonstrate superior invertability. Based on this test, L_{PN}^+ and L_A^+ are more accurate extrapolators than L_N^+ and L_P^+ , and because L_P^+ is the limiting form of explicit finite difference extrapolators, L_{PN}^+ and L_A^+ should be more accurate than explicit finite difference extrapolators as well.

Stability

The singular values of extrapolators L_P^+ , L_N^+ , L_A^+ and L_{PN}^+ are given in Figure 9 for the velocity profile of Figure 3. A depth interval of 100m and a temporal frequency of 40Hz were used. Under recursion, as in depth imaging by downward continuation, singular values not equal to unity in the nonevanescence zone cause nonphysical growth and decay of the wavefield. (Natural amplitude variations must be the result of superposition alone.) As Figure 9 shows, L_P^+ , L_N^+ , L_A^+ and L_{PN}^+ have singular values greater than zero, but those corresponding to L_A^+ and L_{PN}^+ are smaller; L_A^+ is closest to unity. The evanescent boundary occurs at about the 70th singular value, and it is clear that L_A^+ decreases from unity sooner than the rest indicating the potential to be dispersive.

Figures 10a through 11b plot maximum singular value against a range of temporal frequencies and depth intervals (the scales are the same). The values for L_{PN}^+ are smaller than those for L_P^+ and L_N^+ except at the largest depth intervals and temporal frequencies where they are slightly larger. The values for L_A^+ average about 80% the value of the others, indicating that L_A^+ is the most stable extrapolator of the four.

CONCLUSIONS

Taylor series expansion of extrapolated wavefields was used to derive the elementary nonstationary wavefield extrapolators *combination*, and *convolution*. Beginning with the Helmholtz equation (with velocity variation confined to the lateral coordinates) two exact nonstationary filter operators were found for the required second-depth derivative of the recorded wavefield. One is the *convolution* of a nonstationary wavenumber operator with the recorded wavefield, and the other is the *combination* of the recorded spectrum with the same operator. These second-depth derivatives are equivalent in the space and Fourier domains.

Two general formulae for the depth derivatives were deduced from the exact second derivatives. Application to the Taylor series of the formula corresponding to convolution resulted in nonstationary phase shift (NSPS). The combination formula

resulted in phase-shift-plus-interpolation in the nonstationary limit (PSPI). Comparison of the nonstationary extrapolators with commonly implemented ω - x methods demonstrated that PSPI is equivalent to infinite series implementations of ω - x methods. Thus, PSPI is the more accurate one-way extrapolator. There is no commonly implemented ω - x analogue to NSPS.

The relationship between nonstationary extrapolators and *pseudo-differential* operators provided a comparative basis for the exact second derivative and those implied by the two general derivative formulae. The comparison suggested that errors corresponding to nonstationary convolution and combination are complimentary. That is, the average of their vertical wavenumbers tends to increase the order of the error and cancel complex values. A new symmetric extrapolator, and an existing one (i.e., symmetric nonstationary phase shift), that exploit this relationship, were found to be more accurate and more stable than either NSPS or PSPI.

ACKNOWLEDGEMENTS

For his technical assistance, the authors thank Michael Loughlean of Alberta Energy Company (AEC) Ltd. We also thank the sponsors of CREWES for their support of this research.

REFERENCES

- Berkhout, A. J., 1981, Wave field extrapolation techniques in seismic migration, a tutorial: *Geophysics*, **46**, 1638-1656.
- Blacquièrè, G., Debeye, H. W. J., Wapenaar, C. P. A., and Berkhout, A. J., 1989, 3D table-driven migration: *Geophysical prospecting*, **37**, 925-958.
- Claerbout, J. F., 1976, *Fundamentals of geophysical data processing*: McGraw-Hill Book Co., Inc.
- Etgen, J. J., 1994, Stability of explicit depth extrapolation through laterally-varying media: 64th Annual Internat. Mtg., Soc. Expl. Geophys., Expanded Abstracts, 1266-1269.
- Ferguson R. J., and Margrave G. F., 1999, Prestack depth migration by symmetric nonstationary phase shift: mCREWES Research Report, **11**, *This issue*.
- Fishman, L., and McCoy, J. J., 1985, A new class of propagation models based on a factorization of the Helmholtz equation: *Geophys. J. astr. Soc.*, **80**, 439-461.
- Gazdag, J., 1978, Wave equation migration with the phase shift method: *Geophysics*, **43**, 1342 – 1351.
- Gazdag, J., and Sguazero, P., 1984, Migration of seismic data by phase shift plus interpolation: *Geophysics*, **49**, 124 - 131.
- Grimbergen, J. L. T., Dessing, F. J., and Wapenaar, C. P. A., 1998, Modal expansion of one-way operators in laterally varying media: *Geophysics*, **63**, 995-1005.
- Hale, D., 1991a, 3-D depth migration via McClellan transformations: *Geophysics*, **56**, 1778-1785.
- 1991b, Stable explicit extrapolation of seismic wavefields: *Geophysics*, **56**, 1770-1777.
- Holberg, O., 1988, Towards optimum one-way wave propagation: *Geophysical Prospecting*, **36**, 99-114.
- Margrave, G.F., 1998, Theory of nonstationary linear filtering in the Fourier domain with application to time-variant filtering: *Geophysics*, **63**, 244 - 259.
- Margrave, G. F. and Ferguson, R. J., 1997, Wavefield extrapolation by nonstationary phase shift: 67th Annual Internat. Mtg., Soc. Expl. Geophys., Expanded Abstracts, 1599-1602.
- Margrave, G. F. and Ferguson, R. J., 1998, Nonstationary filters, pseudo-differential operators and their inverses: CREWES 11th Annual Research Report, Ch. 26, pp. 1-17.
- 1999, Wavefield extrapolation by nonstationary phase shift: *Geophysics*, **63**, 244 - 259.
- Peterson, B. E., 1983, *Introduction to the Fourier transform and pseudo-differential operators*: Pitman Publishing Limited.

- Soubras, R., 1992, Explicit 3-D migration using equiripple polynomial expansion and Laplacian synthesis: 62nd Annual Internat. Mtg., Soc. Expl. Geophys., Expanded Abstracts, 905-908.
- Stein, E. M., 1993, Harmonic analysis: real-variable methods, orthogonality, and oscillatory integrals: Princeton University Press.
- Stoffa, P. L., Fokkema, J. T., de Luna Freire, R. M., and Kessinger, W. P., 1990, Split-step Fourier migration: *Geophysics*, **55**, 410-421.
- Treves, F., 1980, Introduction to pseudo-differential and Fourier integral operators: Plenum Press.
- Wapenaar, C. P. A., and Grimbergen, J.L.T., 1998, A discussion on stability analysis of wavefield depth extrapolation: 68th Annual Internat. Mtg., Soc. Expl. Geophys., Expanded Abstracts, 1716-1719.
- Wu, R. S., 1992, Scattered field calculation in heterogeneous media using a phase-screen propagator: 62nd Annual Internat. Mtg., Soc. Expl. Geophys., Expanded Abstracts, 1289 - 1292.
- Wu, X. and Wu, R. S., 1998, An improvement to complex screen method for modeling elastic wave reflections: 68th Annual Internat. Mtg., Soc. Expl. Geophys., Expanded Abstracts, 1941-1944.

APPENDIX A

The first term of the integrand in equation (1) is

$$\int \nabla_{\mathbf{x}}^2 \psi(\mathbf{x}, z) \exp(i\mathbf{k} \cdot \mathbf{x}) d\mathbf{x} = \int \exp(i\mathbf{k} \cdot \mathbf{x}) \frac{\nabla_{\mathbf{x}}^2}{(2\pi)^2} \int \varphi(\mathbf{m}, z) \exp(-i\mathbf{m} \cdot \mathbf{x}) d\mathbf{m} d\mathbf{x}, \quad (\text{A1})$$

where ψ is expressed as an inverse Fourier transform of φ . (The notation for ω is suppressed for simplicity.) The Laplacian operates only on the Fourier kernel in equation (A1), and the order of integration can be reversed with the result

$$\int \nabla_{\mathbf{x}}^2 \psi(\mathbf{x}, z) \exp(i\mathbf{k} \cdot \mathbf{x}) d\mathbf{x} = -\frac{1}{(2\pi)^2} \int \mathbf{m} \cdot \mathbf{m} \varphi(\mathbf{m}, z) \int \exp(i\mathbf{x} \cdot [\mathbf{k} - \mathbf{m}]) d\mathbf{x} d\mathbf{m}, \quad (\text{A2})$$

or, recognizing the delta function

$$\begin{aligned} \int \nabla_{\mathbf{x}}^2 \psi(\mathbf{x}, z) \exp(i\mathbf{k} \cdot \mathbf{x}) d\mathbf{x} &= -\frac{1}{(2\pi)^2} \int \mathbf{m} \cdot \mathbf{m} \varphi(\mathbf{m}, z) \delta(\mathbf{k} - \mathbf{m}) d\mathbf{m} \\ &= -\mathbf{k} \cdot \mathbf{k} \varphi(\mathbf{k}, z) \end{aligned} \quad (\text{A3})$$

Replacing spectrum φ with the Fourier transform of ψ gives

$$\int \nabla_{\mathbf{x}}^2 \psi(\mathbf{x}, z) \exp(i\mathbf{k} \cdot \mathbf{x}) d\mathbf{x} = -\mathbf{k} \cdot \mathbf{k} \int \psi(\mathbf{x}, z) \exp(i\mathbf{k} \cdot \mathbf{x}) d\mathbf{x} \quad (\text{A4})$$

Equation (3) can now be written

$$\frac{\partial^2}{\partial z^2} \varphi(\mathbf{k}, z) = -\int k_z^2(\mathbf{x}, \mathbf{k}) \psi(\mathbf{x}, z) \exp(i\mathbf{k} \cdot \mathbf{x}) d\mathbf{x}, \quad (\text{A5})$$

where the square of the vertical wavenumber k_z is

$$k_z^2(\mathbf{x}, \mathbf{k})(\omega) = \left(\frac{\omega}{c(\mathbf{x})} \right)^2 - \mathbf{k} \cdot \mathbf{k} \quad (\text{A6})$$

APPENDIX B

In equation (8), moving the operator in the square brackets inside the Fourier integral is possible due its independence of the wavenumber coordinates \mathbf{k}

$$\frac{\partial^2}{\partial z^2} \psi(\mathbf{x}, z, \omega) = -\frac{1}{(2\pi)^2} \int \varphi(\mathbf{k}, z, \omega) \left[\left(\frac{\omega}{c(\mathbf{x})} \right)^2 \exp(-i\mathbf{k} \cdot \mathbf{x}) - \nabla_{\mathbf{x}}^2 \exp(-i\mathbf{k} \cdot \mathbf{x}) \right] d\mathbf{k} \quad (\text{B1})$$

The Laplacian is thereby applied only to the Fourier kernel

$$\nabla_{\mathbf{x}}^2 \exp(-i\mathbf{k} \cdot \mathbf{x}) = -\mathbf{k} \cdot \mathbf{k} \exp(-i\mathbf{k} \cdot \mathbf{x}) \quad (\text{B2})$$

and the equation for the second depth derivative (B1) becomes

$$\frac{\partial^2}{\partial z^2} \psi(\mathbf{x}, z) = -\frac{1}{(2\pi)^2} \int k_z^2(\mathbf{x}, \mathbf{k}) \varphi(\mathbf{k}, z) \exp(-i\mathbf{k} \cdot \mathbf{x}) d\mathbf{k} \quad (\text{B3})$$

with k_z^2 given by equation (A6).

APPENDIX C

The equivalence of the second depth derivatives, equations (5) and (9), is seen by converting both mixed domain expressions to a single domain. In the Fourier domain, for example, equation (5) requires ψ be replaced with the inverse Fourier transform of φ giving

$$\frac{\partial^2}{\partial z^2} \varphi(\mathbf{k}, z) = \frac{1}{(2\pi)^2} \int \varphi(\mathbf{m}, z) u(\mathbf{k}, \mathbf{m}) d\mathbf{m} \quad (\text{C1})$$

where, for wavenumbers $\mathbf{m} = \{m_x, m_y\}$

$$u(\mathbf{k}, \mathbf{m}) = -\int \left[-\mathbf{k} \cdot \mathbf{k} + \left(\frac{\omega}{c(\mathbf{x})} \right)^2 \right] \exp(i\mathbf{x} \cdot [\mathbf{m} - \mathbf{k}]) d\mathbf{x} \quad (\text{C2})$$

Separating equation (C2) into two terms gives

$$u(\mathbf{k}, \mathbf{m}) = \mathbf{k} \cdot \mathbf{k} \int \exp(i\mathbf{x} \cdot [\mathbf{m} - \mathbf{k}]) d\mathbf{x} - \int \left(\frac{\omega}{c(\mathbf{x})} \right)^2 \exp(i\mathbf{x} \cdot [\mathbf{m} - \mathbf{k}]) d\mathbf{x} \quad (\text{C3})$$

and recognizing the delta function

$$u(\mathbf{k}, \mathbf{m}) = \mathbf{k} \cdot \mathbf{k} \delta(\mathbf{m} - \mathbf{k}) - \int \left(\frac{\omega}{c(\mathbf{x})} \right)^2 \exp(i\mathbf{x} \cdot [\mathbf{m} - \mathbf{k}]) d\mathbf{x} \quad (C4)$$

The Fourier transform of equation (9) is

$$\frac{\partial^2}{\partial z^2} \phi(\mathbf{m}, z) = \frac{1}{(2\pi)^2} \int \phi(\mathbf{k}, z) v(\mathbf{k}, \mathbf{m}) d\mathbf{k} \quad (C5)$$

where

$$v(\mathbf{k}, \mathbf{m}) = - \int \left[-\mathbf{k} \cdot \mathbf{k} + \left(\frac{\omega}{c(\mathbf{x})} \right)^2 \right] \exp(i\mathbf{x} \cdot [\mathbf{m} - \mathbf{k}]) d\mathbf{x} \quad (C6)$$

Using the same process that leads to equation (C2), equation (C6) becomes

$$v(\mathbf{k}, \mathbf{m}) = \mathbf{k} \cdot \mathbf{k} \delta(\mathbf{m} - \mathbf{k}) - \int \left(\frac{\omega}{c(\mathbf{x})} \right)^2 \exp(i\mathbf{x} \cdot [\mathbf{m} - \mathbf{k}]) d\mathbf{x} \quad (C7)$$

Replacement of variables u and v in equations (C1) and (C5) with equations (C4) and (C5) leads to identical results.

APPENDIX D

Applying the first derivative operator, D_+^1 , of equation (10) two times gives an expression for the second derivative

$$\frac{\partial^2}{\partial z^2} \phi(\mathbf{k}, z) \approx \left[D_+^1 \frac{\partial}{\partial z} \psi(\mathbf{x}, z) \right](\mathbf{k}) = \int \pm i k_z(\mathbf{x}, \mathbf{k}) \frac{\partial}{\partial z} \psi(\mathbf{x}, z) \exp(i\mathbf{k} \cdot \mathbf{x}) d\mathbf{x} \quad (D1)$$

and, for general coordinates \mathbf{w} and \mathbf{n} ,

$$k_z(\mathbf{w}, \mathbf{n}) = \sqrt{\left(\frac{\omega}{c(\mathbf{w})} \right)^2 - \mathbf{n} \cdot \mathbf{n}} \quad (D2)$$

The required first derivative $\frac{\partial}{\partial z} \psi$ is approximated as the inverse Fourier transform of the application of D_+^1 given by equation (10)

$$\frac{\partial}{\partial z} \psi(\mathbf{x}, z) \approx \frac{1}{(2\pi)^2} \int [D_+^1 \psi(\mathbf{x}, z)](\mathbf{m}) \exp(-i\mathbf{m} \cdot \mathbf{x}) d\mathbf{m} \quad (D3)$$

The operator in equation (D3) is replaced and equation (D1) becomes

$$\frac{\partial^2}{\partial z^2} \varphi(\mathbf{k}, z) = - \int \psi(\mathbf{y}, z) \frac{1}{(2\pi)^2} \iint k_z(\mathbf{x}, \mathbf{k}) k_z(\mathbf{y}, \mathbf{m}) \exp(i\mathbf{m} \cdot [\mathbf{y} - \mathbf{x}]) \exp(i\mathbf{k} \cdot \mathbf{x}) d\mathbf{m} d\mathbf{x} d\mathbf{y} \quad (D4)$$

Manipulation of equation (D4) into a form similar to the exact second derivative of equation (5) involves the insertion of the term $\exp(i\mathbf{k} \cdot \mathbf{x}) \exp(-i\mathbf{k} \cdot \mathbf{x})$ giving

$$\frac{\partial^2}{\partial z^2} \varphi(\mathbf{k}, z) = - \int \hat{k}_z^2(\mathbf{y}, \mathbf{k}) \psi(\mathbf{y}, z) \exp(i\mathbf{k} \cdot \mathbf{y}) d\mathbf{y} \quad (D5)$$

where

$$\hat{k}_z^2(\mathbf{y}, \mathbf{k}) = \frac{1}{(2\pi)^2} \iint k_z(\mathbf{y}, \mathbf{m}) k_z(\mathbf{x}, \mathbf{k}) \exp(i[\mathbf{m} - \mathbf{k}] \cdot [\mathbf{y} - \mathbf{x}]) d\mathbf{m} d\mathbf{x} \quad (D6)$$

or, under an exchange of coordinates $\mathbf{x} \leftrightarrow \mathbf{y}$ and $\mathbf{k} \leftrightarrow \mathbf{m}$ (so that the output is in space coordinates \mathbf{x} and wavenumbers),

$$\hat{k}_z^2(\mathbf{x}, \mathbf{m}) = \frac{1}{(2\pi)^2} \iint k_z(\mathbf{x}, \mathbf{k}) k_z(\mathbf{y}, \mathbf{m}) \exp(i[\mathbf{k} - \mathbf{m}] \cdot [\mathbf{x} - \mathbf{y}]) d\mathbf{m} d\mathbf{y} \quad (D7)$$

Equation (D7) is a symbol of the *composition* of two pseudo-differential operators. That is, it results from a pseudo-differential operator of the general form

$$[T_c f(\mathbf{x})](\mathbf{k}) = [T_a T_b f(\mathbf{x})](\mathbf{k}) \quad (D7)$$

where T_a and T_b are two pseudo-differential operators with symbols a and b acting on a function f of coordinates \mathbf{x} , and T_c represents an equivalent combination operator with symbol c (Stein, 1993: 238). In equation (D7) symbols a and b correspond to $k_z(\mathbf{x})$ and $k_z(\mathbf{y})$, and symbol c corresponds to $\hat{k}_z^2(\mathbf{x})$. The symbols c of composition operations like equation (D7) have asymptotic formulae (Stein, 1993: 237). For example, beginning with equation (D6), compute the forward Fourier transform over \mathbf{y}

$$\hat{k}_z^2(\mathbf{x}, \mathbf{m}) = \frac{1}{(2\pi)^2} \int k_z(\mathbf{x}, \mathbf{k}) K_z(-[\mathbf{k} - \mathbf{m}], \mathbf{m}) \exp(i\mathbf{x} \cdot [\mathbf{k} - \mathbf{m}]) d\mathbf{k} \quad (D8)$$

where

$$K_z(-[\mathbf{k} - \mathbf{m}], \mathbf{m}) = \int k_z(\mathbf{y}, \mathbf{m}) \exp(-i\mathbf{y} \cdot [\mathbf{k} - \mathbf{m}]) d\mathbf{y} \quad (D9)$$

The replacement of variables $\mathbf{n} = \mathbf{k} - \mathbf{m}$ gives for equation (D8)

$$\hat{k}_z^2(\mathbf{x}, \mathbf{m}) = \frac{1}{(2\pi)^2} \int k_z(\mathbf{x}, \mathbf{m} + \mathbf{n}) K_z(-\mathbf{n}, \mathbf{m}) \exp(i\mathbf{x} \cdot \mathbf{n}) d\mathbf{n} \quad , \quad (\text{D10})$$

or equivalently

$$\hat{k}_z^2(\mathbf{x}, \mathbf{m}) = \frac{1}{(2\pi)^2} \int k_z(\mathbf{x}, \mathbf{m} - \mathbf{n}) K_z(\mathbf{n}, \mathbf{m}) \exp(-i\mathbf{x} \cdot \mathbf{n}) d\mathbf{n} \quad . \quad (\text{D11})$$

Expansion of symbol k_z gives

$$k_z(\mathbf{x}, \mathbf{m} - \mathbf{n}) = k_z(\mathbf{x}, \mathbf{m}) - \mathbf{n} \cdot \nabla_{\mathbf{m}} k_z(\mathbf{x}, \mathbf{m}) + \frac{1}{2} (-\mathbf{n} \cdot \nabla_{\mathbf{m}})^2 k_z(\mathbf{x}, \mathbf{m}) - \dots \quad . \quad (\text{D12})$$

Replacement of k_z in equation (D11) with the above expansion gives

$$\begin{aligned} \hat{k}_z^2(\mathbf{x}, \mathbf{m}) &= k_z(\mathbf{x}, \mathbf{m}) k_z(\mathbf{x}, \mathbf{m}) - \nabla_{\mathbf{m}} k_z(\mathbf{x}, \mathbf{m}) \cdot \frac{1}{(2\pi)^2} \int K_z(\mathbf{n}, \mathbf{m}) \mathbf{n} \exp(-i\mathbf{n} \cdot \mathbf{x}) d\mathbf{n} \\ &+ \frac{1}{(2\pi)^2} \int (\mathbf{n} \cdot \nabla_{\mathbf{m}})^2 k_z(\mathbf{x}, \mathbf{m}) K_z(\mathbf{n}, \mathbf{m}) \exp(-i\mathbf{n} \cdot \mathbf{x}) d\mathbf{n} - \dots \quad . \quad (\text{D13}) \end{aligned}$$

The recognition that $\mathbf{n} \exp(-i\mathbf{n} \cdot \mathbf{x}) \Leftrightarrow -i\nabla_{\mathbf{x}} \exp(-i\mathbf{n} \cdot \mathbf{x})$, leads to the result

$$\begin{aligned} \hat{k}_z^2(\mathbf{x}, \mathbf{m}) &= k_z(\mathbf{x}, \mathbf{m}) k_z(\mathbf{x}, \mathbf{m}) - i\nabla_{\mathbf{m}} k_z(\mathbf{x}, \mathbf{m}) \cdot \nabla_{\mathbf{x}} k_z(\mathbf{x}, \mathbf{m}) \\ &+ \frac{i^2}{2} \nabla_{\mathbf{m}} \nabla_{\mathbf{m}} k_z(\mathbf{x}, \mathbf{m}) : \nabla_{\mathbf{x}} \nabla_{\mathbf{x}} k_z(\mathbf{x}, \mathbf{m}) - \dots \quad , \quad (\text{D14}) \end{aligned}$$

where the third term in equation (D14) is a constant times the product of two-second rank symmetric tensors contracted over both coordinates.

By a similar process, as above, the expression for \bar{k}_z^2 equivalent to equation (D11) is

$$\bar{k}_z^2(\mathbf{x}, \mathbf{m}) = \frac{1}{(2\pi)^2} \int k_z(\mathbf{x}, \mathbf{m} + \mathbf{n}) K_z(\mathbf{n}, \mathbf{m}) \exp(-i\mathbf{x} \cdot \mathbf{n}) d\mathbf{n} \quad . \quad (\text{D15})$$

Equation (D15) differs from (D11) by the positive value of \mathbf{n} ; \mathbf{n} is negative in (D11). The resulting asymptotic formula for \bar{k}_z^2 is

$$\begin{aligned} \bar{k}_z^2(\mathbf{x}, \mathbf{m}) &= k_z(\mathbf{x}, \mathbf{m}) k_z(\mathbf{x}, \mathbf{m}) + i\nabla_{\mathbf{m}} k_z(\mathbf{x}, \mathbf{m}) \cdot \nabla_{\mathbf{x}} k_z(\mathbf{x}, \mathbf{m}) \\ &+ \frac{i^2}{2} \nabla_{\mathbf{m}} \nabla_{\mathbf{m}} k_z(\mathbf{x}, \mathbf{m}) : \nabla_{\mathbf{x}} \nabla_{\mathbf{x}} k_z(\mathbf{x}, \mathbf{m}) + \dots \quad . \quad (\text{D16}) \end{aligned}$$

Asymptotic formulae \bar{k}_z^2 and \hat{k}_z^2 are exact in the first term with all higher terms corresponding to error. The difference in sign of their odd ordered terms suggests that their average will increase the order of the error of the resulting symbol by canceling these terms. Also, because these terms are complex valued, removing them reduces

the presence of uncontrolled complex terms that, in a recursive application, may lead to instability.

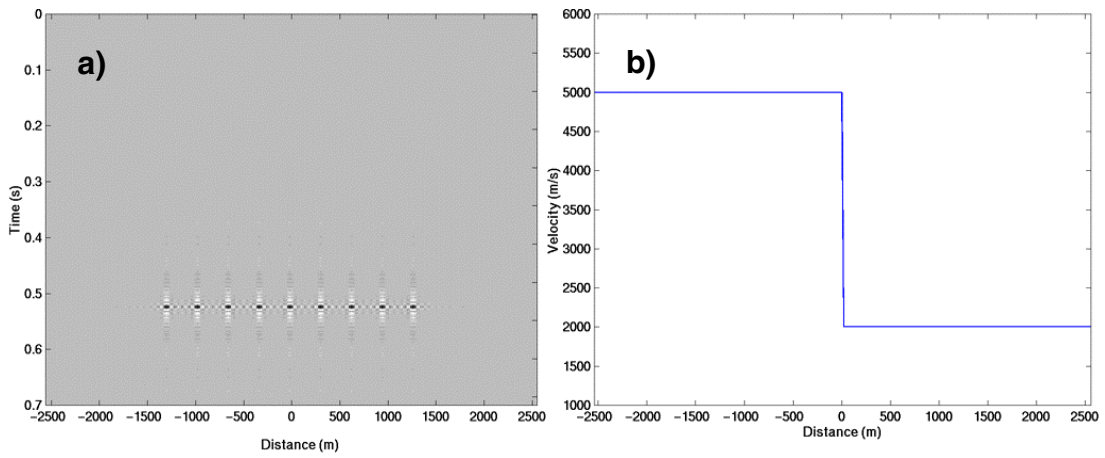


Fig. 1. a) A wavefield of impulses ψ_{imp} (bandlimited in space and time) used to generate impulse responses $L_N^+ \psi_{imp}$, $L_P^+ \psi_{imp}$, $L_{PN}^+ \psi_{imp}$ and $L_A^+ \psi_{imp}$. b) The velocity profile used to generate the impulse responses of Figures 2a, 2b, 6a and 6b.

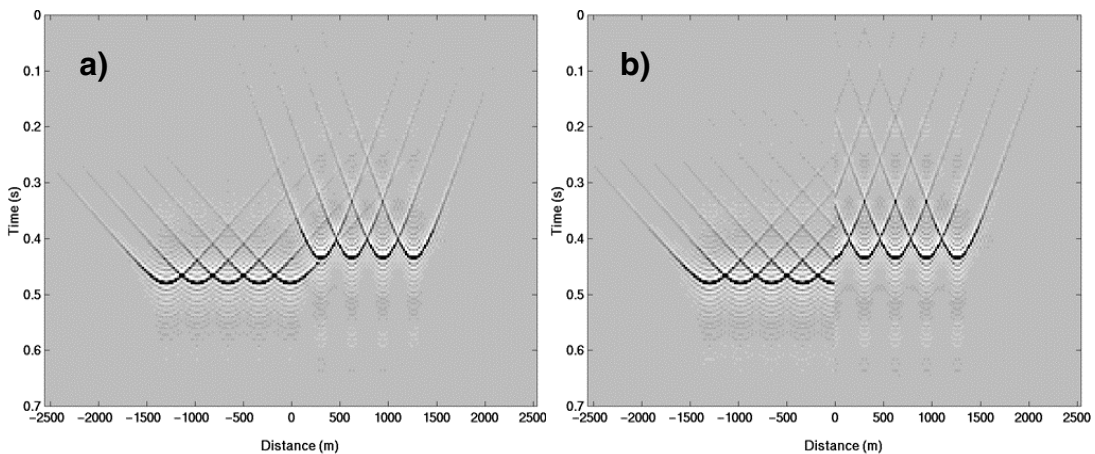


Fig. 2. Impulse responses $L_N^+ \psi_{imp}$ (a) and $L_P^+ \psi_{imp}$ (b) for extrapolation of the data of Figure 1a 200m through the velocity profile of Figure 1b. a) A smooth superposition is characteristic of $L_N^+ \psi_{imp}$. b) A discontinuous superposition is characteristic of $L_P^+ \psi_{imp}$.

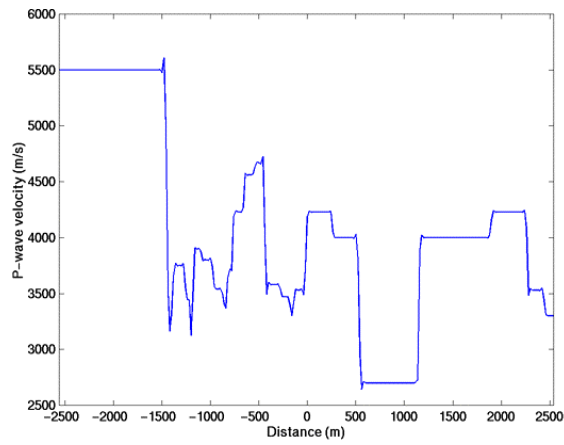


Fig. 3. a) A strongly varying velocity profile used to generate the impulse responses of Figures 4a, 4b, 7a and 7b.

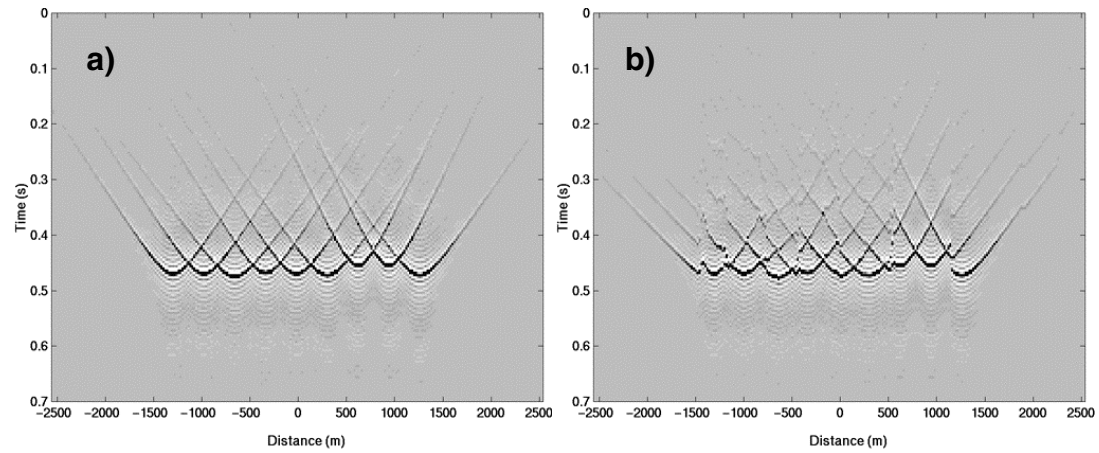


Fig. 4. Impulse responses $L_N^+ \psi_{imp}$ (a) and $L_P^+ \psi_{imp}$ (b) for the velocity profile of Figure 3. The depth interval was 200m. a) The characteristic smooth superposition of $L_N^+ \psi_{imp}$ is retained. b) The characteristic discontinuous superposition for $L_P^+ \psi_{imp}$ is also retained.

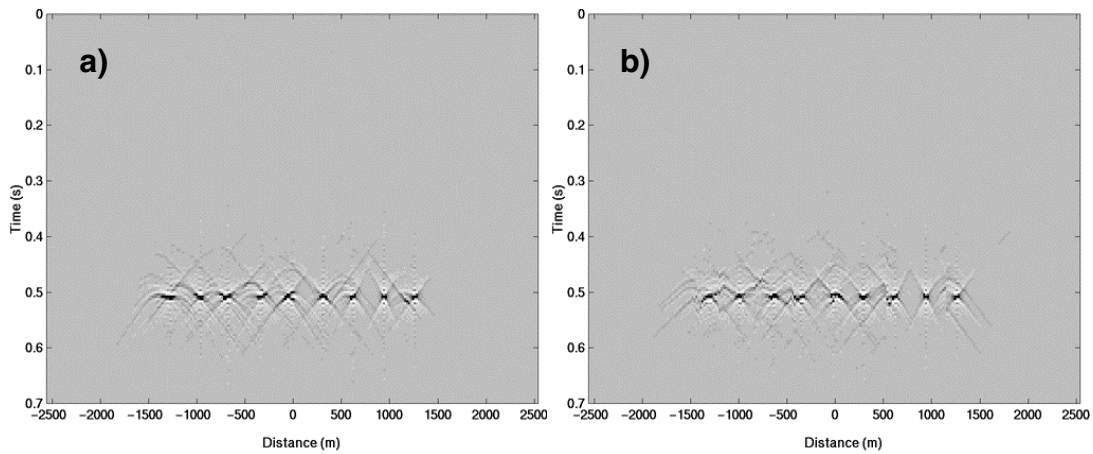


Fig. 5. The impulse responses of Figures 4a and 4b are inverted by extrapolating them – 200m through the velocity profile of Figure 3. a) $L_N^- L_N^+ \psi_{imp}$. b) $L_P^- L_P^+ \psi_{imp}$. Neither inversion does a good job of recovering the input of Figure 1.

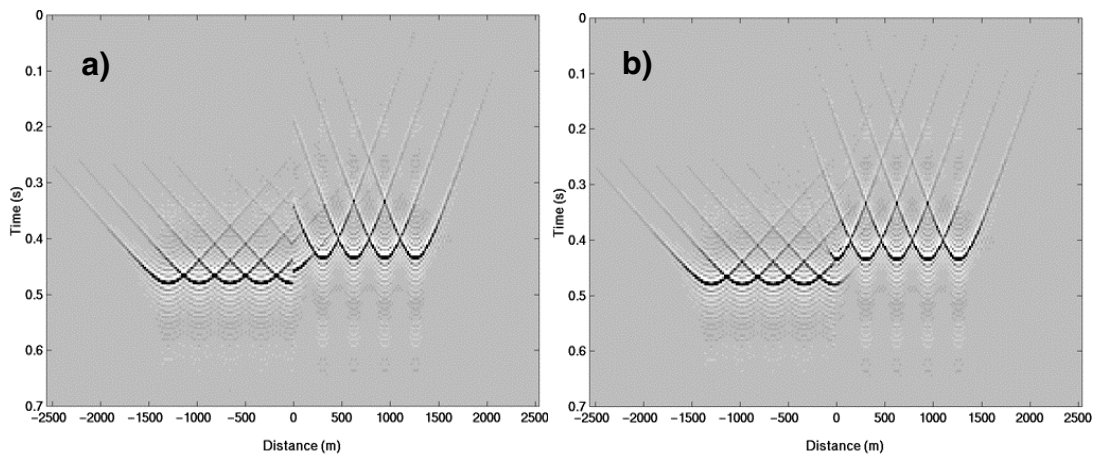


Fig. 6. Impulse responses $L_{PN}^+ \psi_{imp}$ (a) and $L_A^+ \psi_{imp}$ (b) for the data of Figures 1a and 1b. The depth interval was 200m. a) $L_{PN}^+ \psi_{imp}$ combines the truncation effect of $L_P^+ \psi_{imp}$ and the smooth superposition of $L_N^+ \psi_{imp}$. b) Averaging of $L_N^+ \psi_{imp}$ and $L_P^+ \psi_{imp}$ across velocity boundaries is characteristic of $L_A^+ \psi_{imp}$.

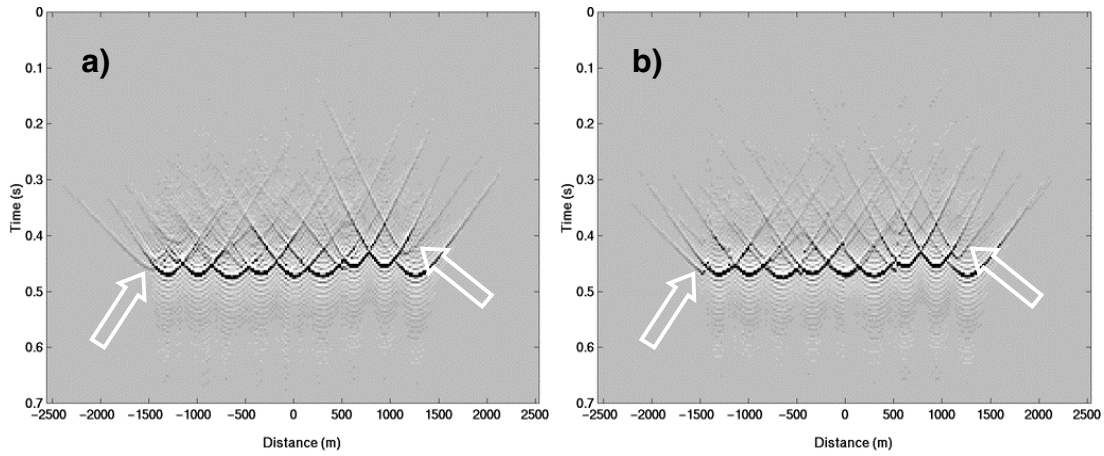


Fig. 7. Impulse responses $L_{PN}^+ \psi_{imp}$ (a) and $L_A^+ \psi_{imp}$ (b) for the velocity profile of Figure 3. The depth interval was 200m. a) The averaging effect of $L_A^+ \psi_{imp}$ is difficult to see due to the complexity of the model. Arrows indicate two of the more obvious averaging characteristics of $L_A^+ \psi_{imp}$ (this is most easily seen in comparison with Figure 7b. b) The combination of the effects of $L_N^+ \psi_{imp}$ and $L_P^+ \psi_{imp}$ characteristic of $L_{PN}^+ \psi_{imp}$ are also difficult to see. Arrows are placed in the same locations as Figure 7a to aid comparison.

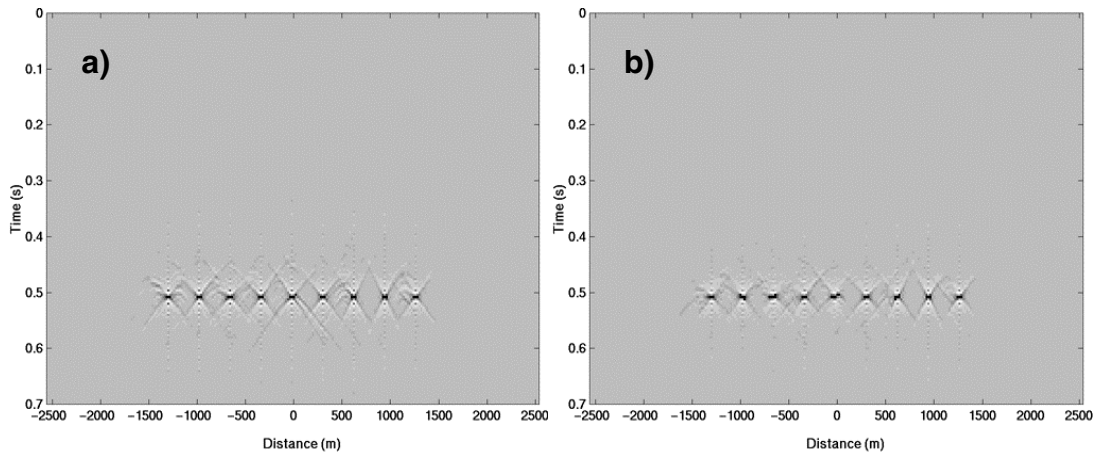


Fig. 8. The impulse responses of Figures 7a and 7b are inverted by extrapolating them – 200m through the velocity profile of Figure 3. a) $L_{PN}^- L_{PN}^+ \psi_{imp}$. b) $L_A^- L_A^+ \psi_{imp}$. Both do a very good job of recovering the input of Figure 1.

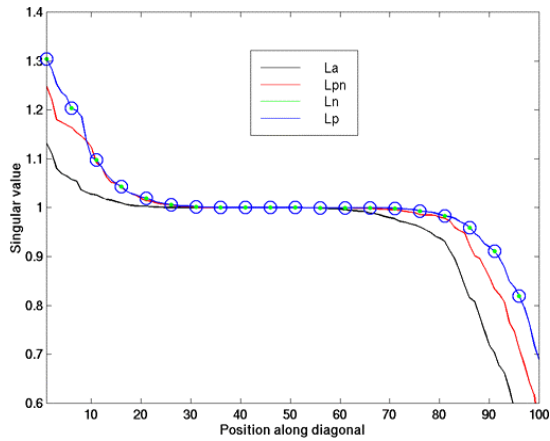


Fig. 9. A comparison of singular values for the velocity profile of Figure 3. The depth interval was 100m and the temporal frequency was 40Hz. The nonevanescence zone corresponds roughly to positions 1 through 70. All four extrapolators have singularities greater than one. During recursion, all four extrapolators will generate nonphysical growth of the wavefield. Extrapolator L_A^+ is the most stable, L_N^+ and L_P^+ exhibit identical stability, and L_{PN}^+ has average stability. The singular values of L_A^+ decrease below unity sooner, as the evanescent boundary approaches, than the others. Thus, L_A^+ may be slightly more dispersive than the rest.

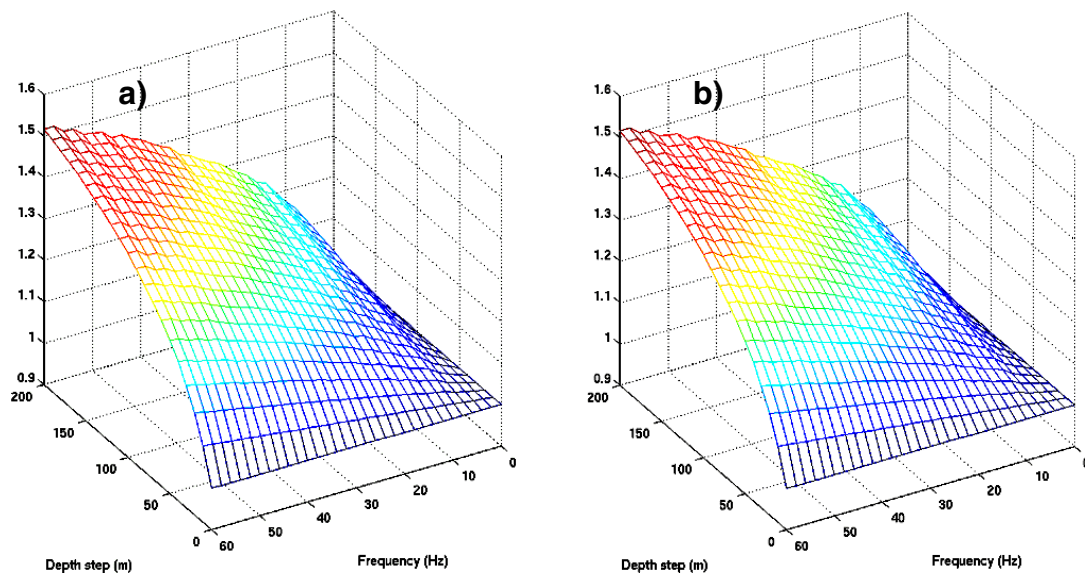


Fig. 10. The maximum singular values of L_N^+ (a) and L_P^+ (b) for the velocity profile of Figure 3. Maximum values for a range of temporal frequency and depth interval are plotted. They are essentially identical.

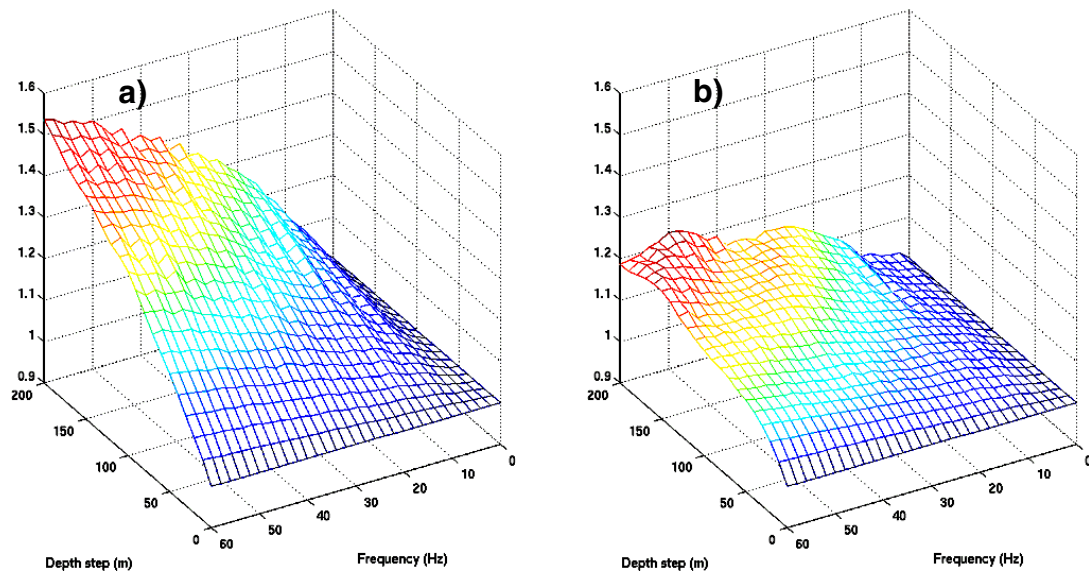


Fig. 11. The maximum singular values of L_{PN}^+ (a) and L_A^+ (b), for the velocity profile of Figure 3, plotted for a range of depth intervals and frequencies. a) The values for L_{PN}^+ are less than those of L_N^+ and L_P^+ every where but at the highest frequencies and largest depth steps. b) Those for L_A^+ average 80% the value of the other extrapolators.